Journal of ELECTRONIC MATERIALS, Vol. 41, No. 9, 2012
DOI: 10.1007/s11664-012-2174-7

AC Conductivity and Diffuse Reflectance Studies of Ag-TiO_2 Nanoparticles

A.K. ABDUL GAFOOR,[1,2] M.M. MUSTHAFA,[1,3] and P.P. PRADYUMNAN[1,4]

1.—Department of Physics, University of Calicut, Malappuram 673635, Kerala, India. 2.—e-mail: gasusmi@gmail.com. 3.—e-mail: mm_musthafa@rediffmail.com. 4.—e-mail: pradyupp@gmail.com

Silver (Ag)-TiO_2 nanoparticles synthesized by a low-temperature hydrothermal method in the anatase phase have been investigated by x-ray diffraction. Transmission electron microscopy has been used for morphological studies. Surface areas were studied by the Brunauer–Emmett–Teller method. Alternating-current (AC) conductivity and dielectric properties were studied for various dopant levels of 0.25 wt.%, 0.5 wt.%, and 1.0 wt.% at 300 K in the frequency range from 42 Hz to 5 MHz. AC conductivity and dielectric properties of TiO_2 nanoparticles were greatly affected by loading with Ag. At high frequencies, the materials showed high AC conductivity and low dielectric constant. Diffuse reflectance studies were carried out for various dopant levels at 300 K by ultraviolet–visible (UV–Vis) spectroscopy. Considerable absorption of visible light by 0.5 wt.% and 1.0 wt.% Ag-TiO_2 nanoparticles was observed due to the decrease of the energy band gap on Ag loading.

Key words: Conductivity, TEM, hydrothermal synthesis, dielectric, spectroscopy

INTRODUCTION

TiO_2 nanoparticles in anatase phase have attracted increasing interest due to their impact in catalytic, optical, and electrical applications. It is a promising material for a variety of problems of environmental interest due to its excellent properties, and it has been studied extensively by various groups.[1–4] The majority of the electrical and optical applications of semiconductor oxides are affected by the presence of various crystalline polymorphs and morphologies.[5] The size-dependent property of semiconductor nanoparticles is important, offering an opportunity to fabricate exotic new devices. Nanotitania is one of the most important ionic semiconductors, with diverse applications in photocatalysis and dye-sensitized solar cells, but it cannot be used as a photocatalyst under light with wavelength above 400 nm due to its wide energy gap (>3.0 eV). It has been reported that doping of metal nanoparticles can enhance the photocatalytic activity of TiO_2 by trapping electrons and thereby hindering recombination of electron–hole pairs.[6] Researchers have paid more attention to stretching its photocatalytically active region to the visible range by incorporating transition and noble metals.[7–10] The present work aims to investigate how loading nanotitania with a noble metal such as silver could change its electrical, dielectric, and optical absorption properties. Anatase-phase TiO_2 nanoparticles have been synthesized by different methods such as the sol–gel method, chemical vapor deposition, the hydrothermal method, and pulsed laser deposition.[11–15] Literature survey revealed that no methods had been reported for synthesis of thermally stable Ag-loaded nanotitania of average particle size 6 nm with enhanced visible light absorption at low temperature. In the present work, 0.25 wt.%, 0.5 wt.%, and 1.0 wt.% Ag-TiO_2 nanomaterials with average particle size of 6 nm were prepared. The dependence of the alternating-current (AC) conductivity of the samples on frequency was studied at room temperature. AC conductivity was found to increase with the frequency of the applied electric field according to the universal power law,[16] and to decrease with increasing silver dopant concentration. The influences of Ag loading

(Received October 25, 2011; accepted June 7, 2012; published online June 27, 2012)

on the optical absorption properties of TiO_2 nanoparticles were also studied. It was observed that loading with silver resulted in significant absorption of light in the visible region, and the percentage absorption increased with increasing Ag dopant level. We have already reported the effect of Sm^{3+} doping on the dielectric properties of TiO_2 nanoparticles.[17]

EXPERIMENTAL PROCEDURES

Analytical-grade titanium(IV) isopropoxide ($Ti[OC_3H_7]_4$) acquired from Acros Organics, and NH_4OH and $AgNO_3$ from Aldrich Chemicals Sigma (99.9% pure grade) were used for the synthesis. Deionized water was used throughout the experiments. NH_4OH solution (50 mL, 5 mol) was added to 7.0 mL titanium(IV) isopropoxide, and the mixture was stirred vigorously for 1 h and then transferred to a stainless-steel Teflon-lined autoclave. The hydrothermal reaction was allowed to proceed at 180°C for 2 h. The synthesized powders were purified with water and acetone and then dried at 80°C. Then, 0.166 g $AgNO_3$ was mixed with 100 mL doubly purified water to form a standard solution. Ten milliliters of this solution was added to 40 mL water and 7.0 mL titanium isopropoxide to achieve 0.25 wt.%, 20 mL of the standard solution was mixed with 30 mL water and 7.0 mL titanium isopropoxide to achieve 0.5 wt.%, and 40 mL of the solution was mixed with 10 mL water and 7.0 mL isopropoxide to achieve 1.0 wt.%. In each case, the hydrothermal reaction was allowed to proceed as before and the synthesized samples were purified and dried at 80°C.

Characterization and Measurements

The x-ray diffraction (XRD) patterns of the samples were recorded using Cu K_α radiation of wavelength 0.15406 nm at scanning rate of 0.02°/s in the 2θ range from 10° to 80°. The Brunauer–Emmett–Teller (BET) specific surface area of the powder was measured using nitrogen adsorption and a surface area analyzer. The particle size and structure were also studied using transmission electron microscopy (TEM). The nanopowders were made in the form of cylindrical pellets of 11 mm diameter and 1 mm thickness by applying a force of about 8 tons for 5 min using a hydraulic press. Dielectric measurements were carried out at room temperature using an impedance analyzer by applying an AC signal across the sample cell with a blocking electrode (silver) in a dielectric cell connected to a computer-controlled HOIKI LCR Hi Tester 3532-50 setup, in the frequency range from 42 Hz to 5 MHz. The real component of the complex dielectric function (ε'), the loss tangent (tan δ), and the AC conductivity (σ_{AC}) were calculated from the measured data using the dimensions of the pellets. Optical studies were carried out using the diffused reflection spectra (DRS) measured by a UV–Vis spectrophotometer.

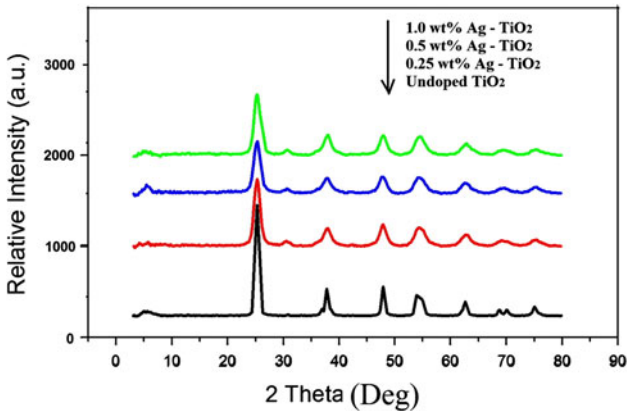

Fig. 1. XRD patterns of undoped TiO_2, 0.25 wt.% Ag-TiO_2, 0.5 wt.% Ag-TiO_2, and 1.0 wt.% Ag-TiO_2 nanoparticles.

RESULTS AND DISCUSSION

XRD Analysis

XRD patterns of Ag-TiO_2 samples are shown in Fig. 1. The observed peaks could be indexed according to the tetragonal structure of anatase TiO_2 (JCPDS, no. 21-1272). All the samples showed high degree of crystallinity, which increased on silver loading without any phase change. Also, there were no obvious peaks showing the presence of silver in the samples, which indicated that silver did not form crystal but rather homogeneously distributed on the surface of TiO_2. The XRD peak broadening on Ag loading was due to the smaller grain size.[18]

The nanocrystallite sizes of the prepared samples were determined using the Debye–Scherrer equation, $D_{XRD} = 0.9\lambda/\beta\cos\theta$, where D is the crystallite size, λ is the x-ray wavelength used, β is the full-width at half-maximum of the XRD diffraction intensity lines, and θ is the half diffraction angle. Table I shows that the crystallite size of the TiO_2 nanoparticles decreased with the silver loading, which is in agreement with earlier reports.[6,18] The present study reveals that loading with silver ions hindered the increase in grain size during hydrothermal synthesis.

Structural Analysis

TEM was carried out for all the samples to establish the grain sizes. Figure 2 shows TEM micrographs of the TiO_2 and Ag-TiO_2 samples, displaying an abundance of spherical particles with average grain diameter in the range of a few nanometers. These images show the uniform nature of the particles with no change in particle morphology due to Ag loading. Also, Ag particles were not identified in the TEM images, as they were well dispersed. The particle size of TiO_2 estimated by TEM was found to be ~16 nm, and that of Ag-TiO_2 samples was found to be ~6 nm. The specific surface area of the powders was measured by the dynamic

Table I. Crystallite sizes, surface areas, and particle sizes of the samples

Samples	Crystallite Size, D_{XRD} (nm)	Specific Surface Area (m^2/g)	Particle Size, D_{BET} (nm)
Undoped TiO_2	16.0	98.6	15.7
0.25 wt.% Ag-TiO_2	6.60	197	7.80
0.5 wt.% Ag-TiO_2	6.50	199	7.75
1.0 wt.% Ag-TiO_2	6.44	200	7.73

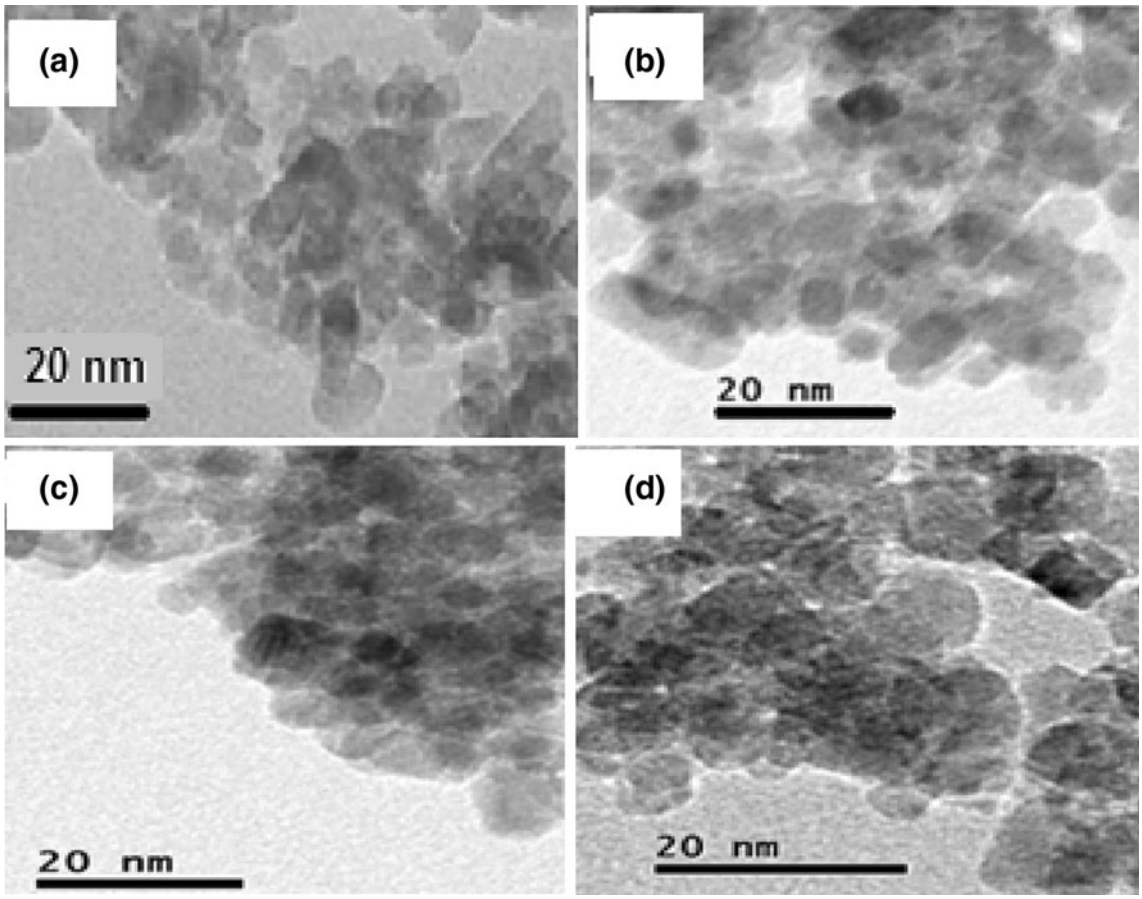

Fig. 2. TEM micrographs of the samples: (a) undoped TiO_2, (b) 0.25 wt.% Ag-TiO_2, (c) 0.5 wt.% Ag-TiO_2, and (d) 1.0 wt.% Ag-TiO_2 nanoparticles.

BET method, in which N_2 gas was adsorbed at 77 K using a Micromeritics system. The surface areas measured for the Ag-loaded samples were higher than that for the pure sample (Table I). The high surface area was due to the reduction of the TiO_2 crystallite size brought about by the silver ions. However, there was only a slightly higher surface area when the Ag content was 1.0 wt.% rather than 0.5 wt.% and 0.25 wt.%. The increase in surface area by Ag doping was reported by Chao et al.[19]

The average particle sizes were calculated from the BET surface area using the equation, $D_{BET} = 6000/\rho S$, where D_{BET} is the average nanoparticle size (nm), ρ is the powder density (g/cm^3), and S is the specific surface area (m^2/g). The results were comparable to the average nanocrystallite size obtained using Scherrer's equation, complementing the TEM findings.

Permittivity and AC Conductivity

The dielectric properties of nanoparticles are influenced by the grain size, cation distribution, synthesis method, etc. Figure 3 shows the variation of dielectric constant (ε') of all samples as a function of frequency at room temperature. The higher values of ε' at lower frequency were due to the simultaneous presence of space charge, dipolar, ionic, and electronic polarizations. At room temperature, in the low-frequency region, the dielectric constant of undoped TiO_2 decreased on doping with Ag due to interfacial charge transfer. Similar results have

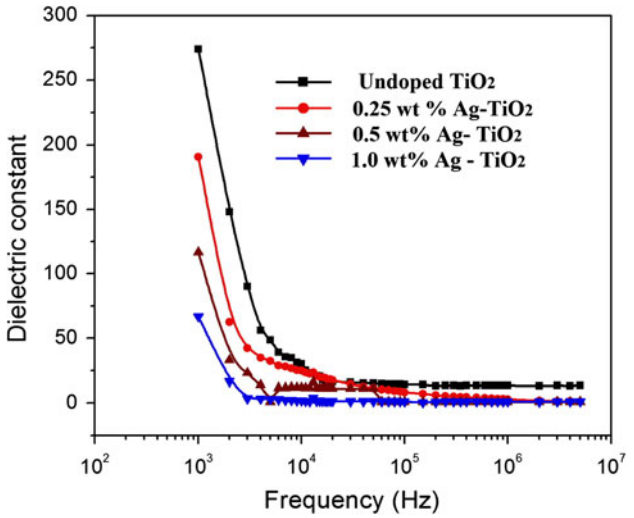

Fig. 3. Variation of dielectric constant of undoped TiO_2, 0.25 wt.% Ag-TiO_2, 0.5 wt.% Ag-TiO_2, and 1.0 wt.% Ag-TiO_2 nanoparticles.

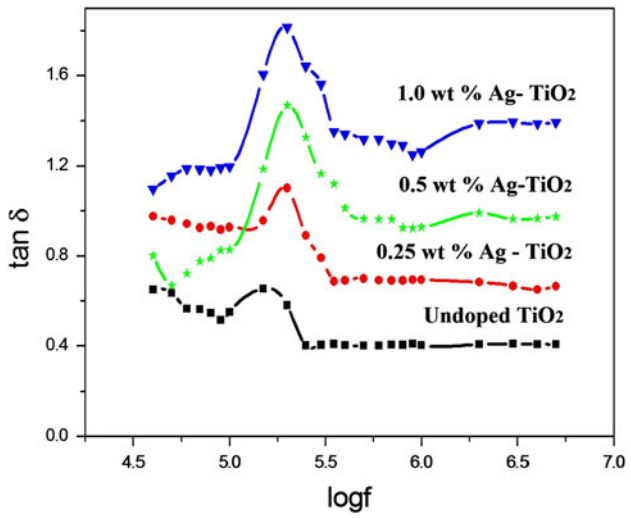

Fig. 4. Variation of loss tangent with frequency for undoped TiO_2, 0.25 wt.% Ag-TiO_2, 0.5 wt.% Ag-TiO_2, and 1.0 wt.% Ag-TiO_2 nanoparticles.

been shown for Fe-, Sm-, and Al-doped nanostructures.[9,20,21] Generally, the dielectric constant (ε') decreases with increasing frequency, but a sudden decrease of dielectric constant (ε') with Ag substitution in the low-frequency region was observed due to the smaller grain size and different polarization mechanism. The polarization in nanomaterials is contributed by space charge polarization, hopping exchange of charge carriers between localized states, and the resultant displacement of dipoles with respect to the applied field. Koops[22] suggested that the effect of grain boundaries is predominant at lower frequencies. Loading of Ag onto TiO_2 thickens the grain boundaries, causing a decrease in the polarization and hence of the dielectric constant (ε'). The nature of the dielectric permittivity related to free dipoles oscillating in an alternating field is as follows: At very low frequencies ($\omega \ll 1/\tau$), where τ is the relaxation time, dipoles follow the field and $\varepsilon' \approx \varepsilon_s$ (the dielectric constant at quasistatic field). As the frequency increases (with $\omega < 1/\tau$), the dipoles begin to lag behind the field and ε' decreases slightly. When the frequency reaches the characteristic frequency ($\omega = 1/\tau$), the dielectric constant drops (relaxation process). At very high frequencies ($\omega \gg 1/\tau$), the dipoles can no longer follow the field and $\varepsilon' = \varepsilon_\infty$ (the high-frequency value of ε'), thus the dielectric constant remains almost constant at high frequencies. This behavior was observed for all the samples. Figure 4 shows the variation of the loss tangent (tan δ) with frequency for all the samples. At lower frequencies, a small abnormal behavior was observed for all the samples due to the collective contribution of charge carriers within the material. The loss spectra were characterized by peaks appearing at characteristic frequencies, suggesting the existence of relaxing dipoles in all the samples. However, the frequency of the tangent loss peak in the Ag-TiO_2 samples was slightly higher than that in the pure sample. However, as the frequency increased, the dielectric relaxation was found to be small and a frequency-independent behavior was observed for all the samples.

The AC conductivity (σ_{AC}) of the samples was calculated using the dielectric equation $\sigma_{AC} = \omega\varepsilon_0\varepsilon_r \tan\delta$, where ω is the angular frequency and ε_0 is the permittivity of free space. Figure 5 shows the variation of the AC conductivity as a function of frequency for the samples at room temperature. It was observed that, in all the samples, the AC conductivity was constant up to 100 kHz but increased steeply thereafter, as in disordered materials such as polypyrrole and Ni-TiO_2 crystals.[23,24] Also, at higher frequencies, the AC conductivity of TiO_2 was reduced by Ag loading. As the particle size decreased, the surface-to-volume ratio increased and large surface scattering occurred, which resulted in a reduction in the electronic conductivity.[23] The high conductivity at higher frequencies confirms the short-range intrawell hopping of charge carriers between localized states. However, on loading with silver, the effective number of charge carriers involved in the doping mechanism was decreased, and hence the conductivity was found to decrease.

UV–Visible Diffuse Reflectance Spectra

Figure 6 shows the optical absorption spectra of undoped TiO_2 and Ag-doped TiO_2 nanoparticles obtained by UV–Vis diffuse reflectance (DRS) in the range from 200 nm to 900 nm. The undoped TiO_2 showed a broad absorption in the UV region below 400 nm due to electron transfer from the valence band (2p orbitals of oxide anion) to the conduction band (3dt_2g orbitals of Ti^{4+} cation). It is also inferred that the absorption rate increased with increasing percentage of Ag, and a strong absorption around 450 nm to 600 nm in the visible region was shown

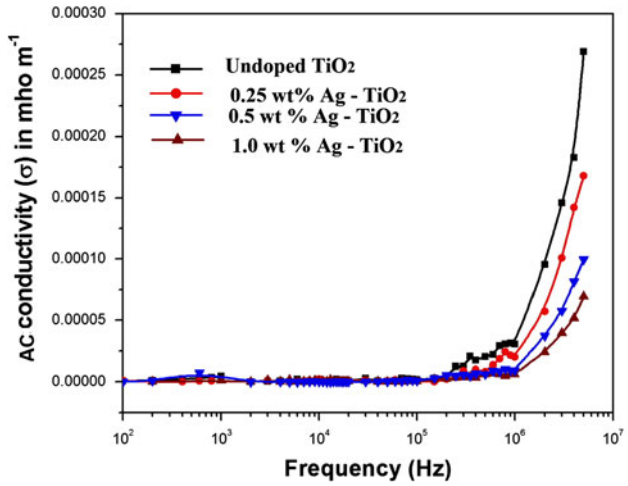

Fig. 5. Variation of AC conductivity with frequency for undoped TiO_2, 0.25 wt.% Ag-TiO_2, 0.5 wt.% Ag-TiO_2, and 1.0 wt.% Ag-TiO_2 nanoparticles.

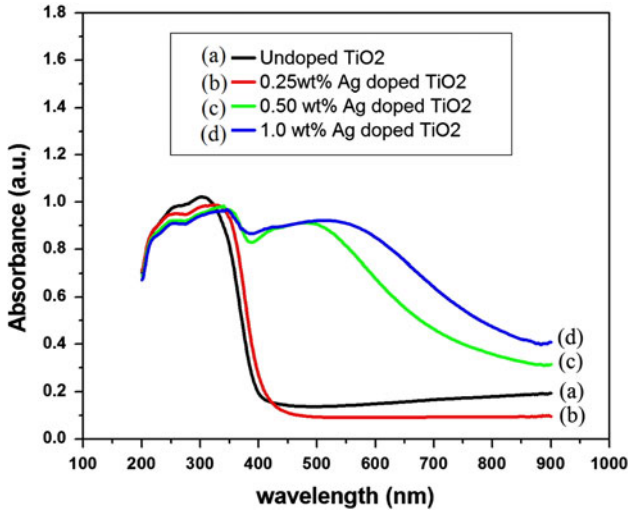

Fig. 6. DRS of undoped TiO_2, 0.25 wt.% Ag-TiO_2, 0.5 wt.% Ag-TiO_2, and 1.0 wt.% Ag-TiO_2 nanoparticles.

by 0.5 wt.% and 1.0 wt.% Ag-TiO_2 nanoparticles. This could result from the introduction of localized energy levels by silver clusters in the band gap of TiO_2, into which valence-band electrons were excited at wavelength longer than 400 nm. It is clear from the sample characterizations that the Ag ions are highly dispersed on the TiO_2, and this increase of metal dispersion resulted in increased interaction between Ag and TiO_2 particles, leading to broadening of absorption. Similar studies on the effects of particle size, size distribution, and surface coverage of Ag-TiO_2 nanoparticles on visible light absorption have been reported.[25,26]

CONCLUSIONS

TiO_2 and Ag-TiO_2 nanocrystals in anatase phase were synthesized by a low-temperature hydrothermal method. XRD, BET surface area, and TEM analyses confirmed that the Ag loading resulted in the reduction of the crystallite size of TiO_2 from 16 nm to 6 nm without any phase change. The TiO_2 nanoparticles had high dielectric constant and displayed an abnormal dielectric behavior in the low-frequency region. The presence of Ag reduced the dielectric constant and AC conductivity and shifted the dielectric loss peak to higher-frequency region. At higher frequencies, the dielectric constant was found to be constant and low, but the AC conductivity increased rapidly. Also, loading of Ag into the TiO_2 remarkably enhanced the visible light absorption, and the rate of absorption increased with increasing Ag content. This property of the materials could therefore be used for dielectric and optical applications.

ACKNOWLEDGEMENTS

A.K.A.G. gratefully acknowledges the University Grants Commission, Government of India, for the award of a research fellowship under the Faculty Improvement Programme (FIP).

REFERENCES

1. S.W. Kim, T.H. Han, J. Kim, H. Gwon, H.S. Moon, S.W. Kang, S.O. Kim, and K. Kang, *ACS Nano* 3, 1085 (2009).
2. D. Kuang, J. Brillet, P. Chen, M. Takata, S. Uchida, H. Miura, K. Sumioka, S.M. Zakeeruddin, and M. Gratzel, *ACS Nano* 2, 1113 (2008).
3. K. Shankar, J. Bandara, M. Paulose, H. Wletash, O.K. Varghese, G.K. More, M. Thelakkat, and C.A. Grimes, *Nanoletters* 8, 1654 (2008).
4. J. Thomas, K. Praveen Kumar, and S. Mathew, *Sci. Adv. Mater.* 2, 481 (2010).
5. C. Lee, P. Ghosez, and X. Gonze, *Phys. Rev. B* 50, 13379 (1994).
6. S. Ko, C.K. Banerjee, and J. Sankar, *Compos. B* 42, 579 (2011).
7. C. He, Y. Yu, X.F. Hu, and A. Larbot, *Appl. Surf. Sci.* 200, 238 (2002).
8. N. Sobana, M. Muruganadham, and M. Swaminathan, *J. Mol. Catal. A* 258, 124 (2006).
9. Q. Chen, W. Shi, Y. Xu, D. Wu, and Y. Sun, *Mater. Chem. Phys.* 1251, 825 (2011).
10. J. Garcia-Serrano, E. Gomez-Hernandez, M. Ocampo-Fernandez, and U. Pal, *Curr. Appl. Phys.* 9, 1097 (2009).
11. T. Trung, W.J. Cho, and C.S. Ha, *Mater. Lett.* 57, 2746 (2003).
12. C.H. Lu and M.C. Wen, *J. Alloys Compd.* 448, 153 (2008).
13. B. Jiang, H. Yin, T. Jiang, J. Yan, Z. Fan, C. Li, J. Wu, and Y. Wada, *Mater. Chem. Phys.* 92, 595 (2005).
14. D. Byun, Y. Jin, B. Kim, J.K. Lee, and D. Park, *J. Hazard. Mater.* 73, 199 (2000).
15. E. Gyorgy, G. Socol, E. Axente, I.N. Mihailescu, C. Ducu, and S. Cluca, *Appl. Surf. Sci.* 247, 429 (2005).
16. K. Funke, *Prog. Solid State Chem.* 22, 111 (1993).
17. A.K. Abdul Gafoor, J. Thomas, M.M. Musthafa, and P.P. Pradyumnan, *J. Electron. Mater.* 40, 2152 (2011).
18. S. Mona and M.S.A. Abdel-Mottaleb, *Inorg. Chem. Acta* 360, 2863 (2007).
19. H.E. Chao, Y.U. Yun, H.U. Xingfang, A. Larbot, and Euro, *J. Eur. Ceram. Soc.* 23, 1457 (2003).
20. D. Singh, P. Yadev, N. Singh, C. Kant, M. Kumar, S.D. Sharma, and K.K. Saini, *J. Exp. NanoSci.* (2011). doi: 10.1080/17458080.2011.564215.
21. A.T. Raghavender and K.M. Jadev, *Bull. Mater. Sci.* 32, 575 (2009).
22. C. Koops, *Phys. Rev.* 83, 121 (1951).

23. K. Karthik, S. Kesavapandian, and N. Victor Jaya, *Appl. Surf. Sci.* 256, 6829 (2010).
24. I. Sakellis, A.N. Papathanassiou, and J. Grammatikakis, *Appl. Phys. Lett.* 97, 042904 (2010).
25. M.S. Lee, S.-S. Hong, and M. Mohseni, *J. Mol. Catal. A* 242, 135 (2005).
26. J. Yu, J. Xiong, B. Cheng, and S. Liu, *Appl. Catal. B* 60, 211 (2005).